



Preparation of classical $\text{Re}^{99\text{mTc}(\text{CO})_3^+}$ and novel $^{99\text{mTc}(\text{CO})_2(\text{NO})^{2+}}$ cores complexed with flavonol derivatives and their binding characteristics for $\text{A}\beta_{(1-40)}$ aggregates

Yang Yang, Lin Zhu, Mengchao Cui, Ruikun Tang, Huabei Zhang*

Key Laboratory of Radiopharmaceuticals, Ministry of Education, College of Chemistry, Beijing Normal University, Beijing 100875, PR China

ARTICLE INFO

Article history:

Received 26 November 2009

Revised 28 January 2010

Accepted 9 April 2010

Available online 31 July 2010

Keywords:

$\text{A}\beta_{(1-40)}$ aggregates

$\text{Re}^{99\text{mTc}(\text{CO})_3^+}$ -3-OH-flavone

$^{99\text{mTc}(\text{CO})_2(\text{NO})^{2+}}$

Autoradiography

K_d

Fluorescence

UV-spectra

Biodistribution

ABSTRACT

Classical $^{99\text{mTc}(\text{CO})_3^+}$ and novel $^{99\text{mTc}(\text{CO})_2(\text{NO})^{2+}}$ cores complexed with flavonol derivatives were prepared. Autoradiography of postmortem AD transgenic mice (Tg C57, APP, PS1 12-month-old) brain section confirmed the binding property of $^{99\text{mTc}(\text{CO})_3^+}$ -3-OH-flavone⁰ to $\text{A}\beta_{(1-40)}$ aggregates, while the novel $^{99\text{mTc}(\text{CO})_2(\text{NO})^{2+}}$ labeled compounds showed no binding sites in AD transgenic mice sections. Intravenous administration of $^{99\text{mTc}(\text{CO})_3^+}$ -3-OH-flavone⁰ resulted in moderate brain uptake ($0.48 \pm 0.05\%$ ID/g) at 5 min post-injection and slow clearance from the brain issues in 2 h post-injection (120 min: $0.39 \pm 0.08\%$ ID/g). Then an $\text{A}\beta_{(1-40)}$ -receptor-targeted $\text{Re}(\text{CO})_3^+$ -3-OH-flavone, was prepared to identify the structure of the technetium complex. UV-vis absorption and fluorescence emission properties have been studied at room temperature in order to determine the natures of the lowest electronically excited states of $\text{Re}(\text{CO})_3^+$ -3-OH-flavone and the ligand. The fluorescent rhenium complex $\text{Re}(\text{CO})_3^+$ -3-OH-flavone showed high affinity for $\text{A}\beta_{(1-40)}$ aggregates in vitro by fluorescence spectra (dissociation constant (K_d) = 11.16 nM). In conclusion, the results suggested that $^{99\text{mTc}(\text{CO})_3^+}$ -3-OH-flavone should be a suitable candidate as $\text{A}\beta$ plaque SPECT imaging agent for AD.

Crown Copyright © 2010 Published by Elsevier Ltd. All rights reserved.

Alzheimer's disease (AD) caused 50–60% of all the dementia cases, and it is a brain disorder associated with progressive memory loss and decrease of cognitive function.¹ In the development and progression of AD, the formation of the senile plaques are critical factors, and the senile plaques are extracellular deposits of amyloid fibrils of β -amyloid ($\text{A}\beta$) ($\text{A}\beta_{(1-40)}$ and $\text{A}\beta_{(1-42)}$),² the characteristic of which was a typical β -sheet form.^{3,4} However, early diagnosis of AD is often unreliable and the only definitive confirmation of AD is by postmortem histopathological examination of amyloid deposits in the brain.⁵ Thus, the direct mapping of $\text{A}\beta$ aggregates in the living brain by PET and SPECT $\text{A}\beta$ aggregates-specific imaging agents is an active research area. Many agents has been attempted and several of them might be selected as the candidates for targeting $\text{A}\beta$ aggregates, such as ^{18}F -FDDNP,⁶ ^{11}C -PIB,⁷ and ^{11}C -SB-13.⁸ Currently, novel radioiodinated flavone derivatives for imaging of β -amyloid plaques were reported by Masahiro Ono,^{9,10} and the binding affinities of radioiodinated flavones were from 13 to 77 nM. In addition, these compounds displayed high brain uptakes at 2 min post-injection and rapid wash-out from the brain at 30 min in normal mice. The reports suggested that these flavone derivatives might be candidates for β -amyloid aggregates imaging.

However, the development of $^{99\text{mTc}}$ -labeled radioactive probes for SPECT was lagging far behind. Technetium-99m labeled compounds would be particularly useful in view of the favorable physical properties ($t_{1/2} = 6$ h, $E_\gamma = 140$ keV), easy and widespread availability, and low cost of the $^{99\text{mTc}}$ nuclide as well.¹¹ Since there is no stable isotope of Tc available, the use of rhenium, as a VIIB congener of technetium, may facilitate the development of technetium-99m labeled complexes, because of the similar physical, chemical and biodistribution properties of the two nuclides. Moreover, the methodologies developed to generate Re complexes are generally applicable to generate their corresponding Tc analogs, so rhenium complexes were often used as a non-radioactive alternative for the structural characterization of technetium complexes and the determination of binding affinities of the Tc-radiotracers.¹²

Here to fore, no $^{99\text{mTc}}$ -labeled compound has been successfully applied for $\text{A}\beta$ aggregates imaging due to the low penetration into blood–brain barrier (BBB), in spite of their high binding affinities for $\text{A}\beta$ aggregates.^{13–16} However, the classical $^{99\text{mTc}(\text{CO})_3^+}$ and novel $^{99\text{mTc}(\text{CO})_2(\text{NO})^{2+}}$ cores were helpful to design new radiopharmaceuticals, and in our previous report, we have successfully converted the $^{99\text{mTc}(\text{CO})_3^+}$ core into $^{99\text{mTc}(\text{CO})_2(\text{NO})^{2+}}$ with $[\text{NO}][\text{BF}_4]$ in water and acetonitrile.¹⁷

Thus, in order to develop $^{99\text{mTc}}$ labeled $\text{A}\beta$ plaques imaging agents, we prepared novel $\text{Re}^{99\text{mTc}(\text{CO})_3^+}$ -complexed 3-OH-flavone and $^{99\text{mTc}(\text{CO})_2(\text{NO})^{2+}}$ core labeled 6-OH-flavone

* Corresponding author. Tel.: +86 10 58802961.

E-mail address: hbzhang@bnu.edu.cn (H. Zhang).

(7-OH-flavone) derivatives. Moreover, since Klunk W. E.¹⁸ and H. LeVine III etc.¹⁹ reported the determination of the values of K_d by

fluorescence spectra, there has been few report on the same method used to measure the values of K_d when $\text{Re}(\text{CO})_3^+$ -compounds

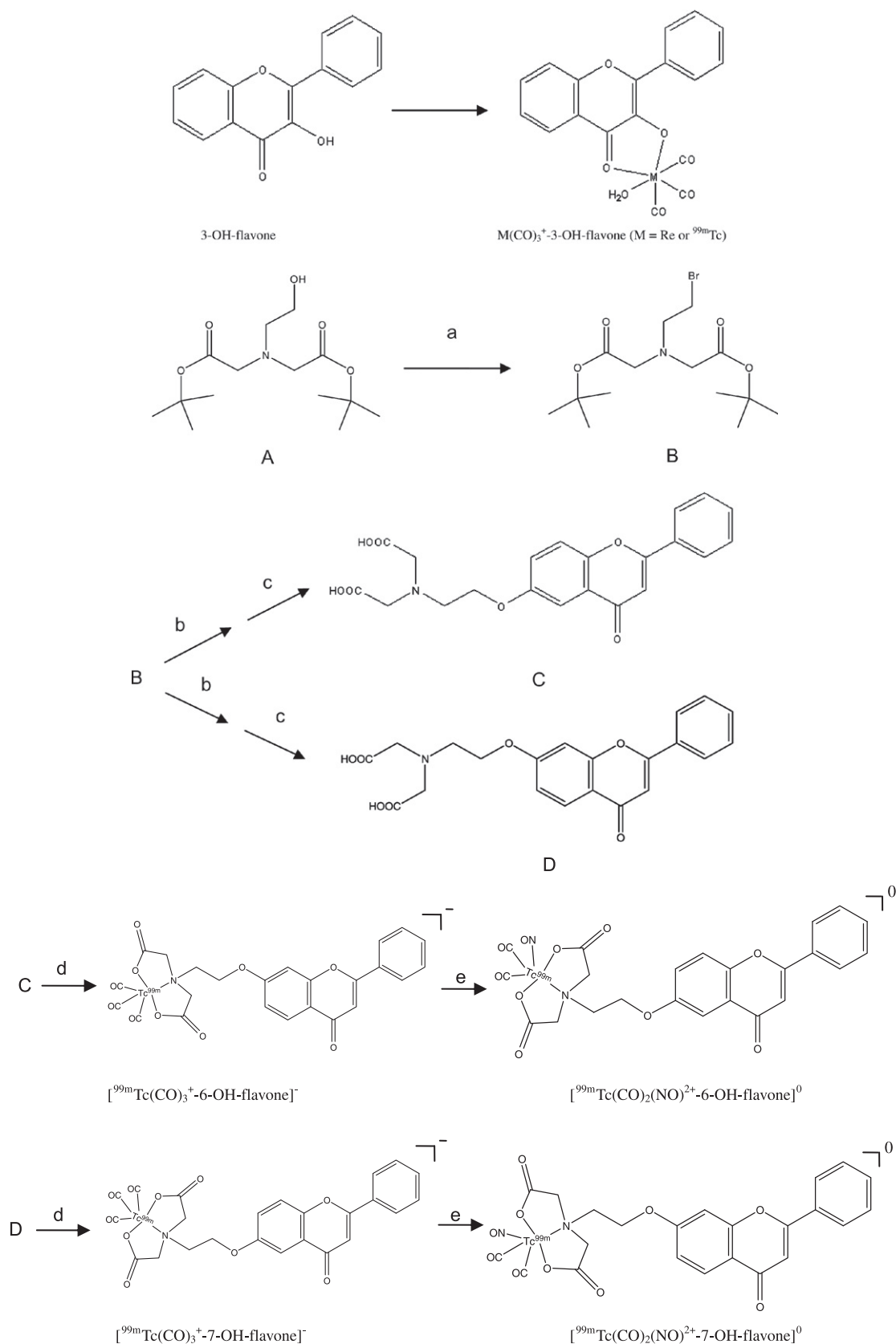


Figure 1. Reagents and conditions: $\text{Re}(\text{CO})_5\text{Br}$, KOH, H_2O , reflux, 22 h ($\text{Re}(\text{CO})_3^+$ -3-OH-flavone); [$^{99\text{m}}\text{Tc}(\text{CO})_3(\text{H}_2\text{O})$]⁺, H_2O , pH 11, 100 °C, 40 min ($^{99\text{m}}\text{Tc}(\text{CO})_3^+$ -3-OH-flavone); (a) Ph_3P , NBS, CH_2Cl_2 ; (b) 6-OH-flavone(7-OH-flavone), KOH, ethanol; (c) CF_3COOH , CH_2Cl_2 ; (d) [$^{99\text{m}}\text{Tc}(\text{CO})_3(\text{H}_2\text{O})$]⁺, H_2O , pH 11, 100 °C, 100 min; (e) NOBF_4 , H_2O , pH 1, 100 °C, 15 min.

binding to A β aggregates. So the novelty of this research is to establish a credible method by fluorescence spectra in the measurement of K_d of the $\text{Re}(\text{CO})_3^+$ -complexed 3-OH-flavone, and this method was based on the factor that when A β aggregates was added to the solution of a small molecule, the quantum yield of fluorescence of the molecule may be increased because the rotation of the rings about one another upon transition to the excited state is inhibited by the rigidity of the micro surrounding of the aggregates.^{20,21}

In this work, classical $^{99\text{m}}\text{Tc}(\text{CO})_3^+$ core labeled 3-OH-flavone and novel $^{99\text{m}}\text{Tc}(\text{CO})_2(\text{NO})^{2+}$ core labeled 6-OH-flavone (7-OH-flavone) derivatives were prepared. $[\text{Re}(\text{CO})_3^+-3\text{-OH-flavone}]^0$ labeled the AD mice (Tg C57, APP, PS1 12-month-old) brain section in comparison to the no binding sites in the normal mice section by autoradiography, oppositely, the $^{99\text{m}}\text{Tc}(\text{CO})_2(\text{NO})^{2+}$ complexes did not label the AD mice brain section, so we did not synthesize the $\text{Re}(\text{CO})_2(\text{NO})^{2+}$ complexes, but the $\text{Re}(\text{CO})_3^+-3\text{-OH-flavone}$ was synthesized to identify the structure of the Tc-99m complex, and the rhenium complex with affinity for A $\beta_{(1-40)}$ aggregates in vitro was determined to be 11.16 nM by fluorescence spectra in vitro. Then,

the biological characterization of $[\text{Re}(\text{CO})_3^+-3\text{-OH-flavone}]^0$ in normal mice was also performed to evaluate its potential as a tracer for visualization of β -amyloid plaques.

The preparation routes of $\text{Re}/^{99\text{m}}\text{Tc}(\text{CO})_3^+-3\text{-OH-flavone}$, $[\text{Re}(\text{CO})_2(\text{NO})^{2+}-6\text{-OH-flavone}]^0$ and $[\text{Re}(\text{CO})_2(\text{NO})^{2+}-7\text{-OH-flavone}]^0$ are shown in Figure 1.

The compound $\text{Re}(\text{CO})_3^+-3\text{-OH-flavone}$ was obtained as a light yellow solid (yield 78%) via a one-stage reaction,^{25a} and the $[\text{Re}(\text{CO})_3^+-3\text{-OH-flavone}]^0$ was prepared via $[\text{Re}(\text{CO})_3^+(\text{H}_2\text{O})_3]^+$ moiety²² by direct labeling method,^{25c} as outlined in Figure 1. The chemical identities of $\text{Re}(\text{CO})_3^+-3\text{-OH-flavone}$ were confirmed by NMR,²⁶ MS-ESI²⁷ and Infrared Spectrum.²⁸ The labeling yield of $[\text{Re}(\text{CO})_3^+-3\text{-OH-flavone}]^0$ detected by radio-TLC²⁹ was higher than 95%, and the R_f s of $^{99\text{m}}\text{Tc}(\text{CO})_3^+-3\text{-OH-flavone}$ and $[\text{Re}(\text{CO})_3^+(\text{H}_2\text{O})_3]^+$ were 0.6–0.7 and 0–0.1, respectively (Table 1). The radio-chemical purity was higher than 92% by reversed phase HPLC.^{30a} Moreover, $[\text{Re}(\text{CO})_3^+-3\text{-OH-flavone}]^0$ was proved to be neutral by paper electrophoresis³¹ (Table 3). The identity of the radioactive complex was established by comparative HPLC^{30a}

Table 1

The distributions of radioactivity of $[\text{Re}(\text{CO})_3^+-3\text{-OH-flavone}]^0$ (A) and $[\text{Re}(\text{CO})_3^+(\text{H}_2\text{O})_3]^+$ (B)

R_f	0	0.1	0.2	0.3	0.4	0.5	0.6	0.7	0.8	0.9
A	15,570	29,857	16,423	8045	10,117	36,979	139,554	102,281	8744	14,316
B	394,875	122,797	79,281	35,401	29,781	28,547	36,444	27,662	29,436	43,257

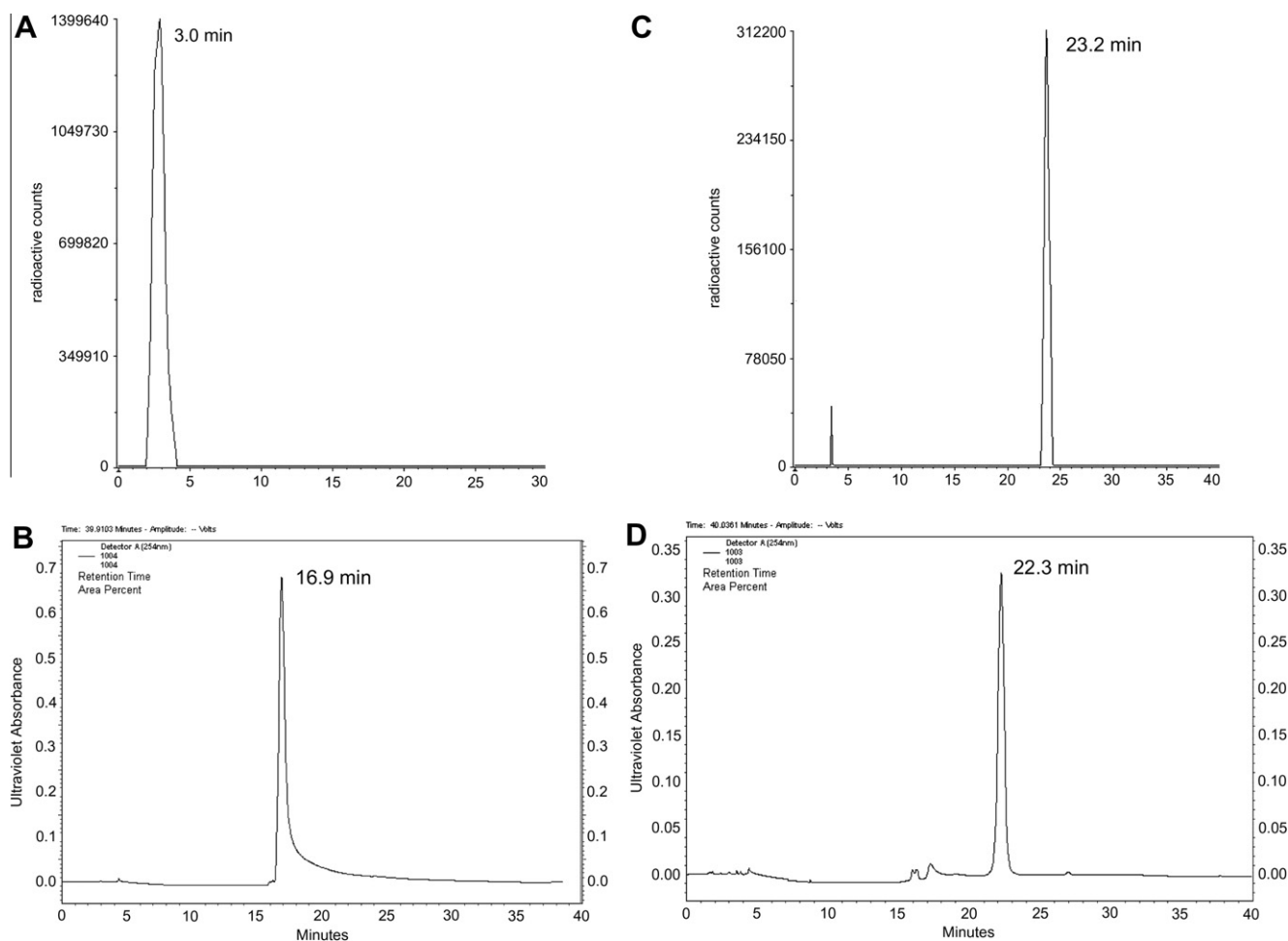


Figure 2. The HPLC chromatograms of $[\text{Re}(\text{CO})_3^+(\text{H}_2\text{O})_3]^+$ (A), 3-OH-flavone (B), $[\text{Re}(\text{CO})_3^+-3\text{-OH-flavone}]^0$ (C) and $\text{Re}(\text{CO})_3^+-3\text{-OH-flavone}$ (D).

Table 2

The distributions of radioactivity of $[^{99m}\text{Tc}(\text{CO})_3(\text{H}_2\text{O})_3]^+$ (A), $[^{99m}\text{Tc}(\text{CO})_3^+-6\text{-OH-flavone}]^-$ (B), $[^{99m}\text{Tc}(\text{CO})_3^+-7\text{-OH-flavone}]^-$ (C), $[^{99m}\text{Tc}(\text{CO})_2(\text{NO})^{2+}-6\text{-OH-flavone}]^0$ (D) and $[^{99m}\text{Tc}(\text{CO})_2(\text{NO})^{2+}-7\text{-OH-flavone}]^0$ (E)

R_f	0	0.1	0.2	0.3	0.4	0.5	0.6	0.7	0.8	0.9
A	4578	95	81	103	87	91	94	96	116	104
B	98	103	147	92	87	644	329	101	92	91
C	78	129	133	98	96	782	291	132	101	77
D	278	1642	85	103	80	78	82	95	91	112
E	149	798	84	97	99	101	81	85	87	101

studies using the corresponding rhenium complex as reference. The retention times for $\text{Re}(\text{CO})_3^+-3\text{-OH-flavone}$ (UV) and $[^{99m}\text{Tc}(\text{CO})_3^+-3\text{-OH-flavone}]^0$ (radioactivity) on HPLC^{30a} were 22.3

Table 3

Electrophoresis pattern of $[^{99m}\text{Tc}(\text{CO})_3^+-3\text{-OH-flavone}]^0$ (A), $[^{99m}\text{Tc}(\text{CO})_2(\text{NO})^{2+}-6\text{-OH-flavone}]^0$ (B) and $[^{99m}\text{Tc}(\text{CO})_2(\text{NO})^{2+}-7\text{-OH-flavone}]^0$ (C)

	Position	Cathode	Origin	Anode
A	Radioactive counts	596	9673	475
B	Radioactive counts	936	11,875	539
C	Radioactive counts	441	9843	338

(Fig. 2D) and 23.2 min (Fig. 2C), respectively, in comparison to the ligand 3-OH-flavone (UV-HPLC, ^{30a} 16.9 min, Fig. 2B) and precursor $[^{99m}\text{Tc}(\text{CO})_3(\text{H}_2\text{O})_3]^+$ (radio-HPLC, ^{30a} 3.0 min, Fig. 2A), respectively. The retention time of $[^{99m}\text{Tc}(\text{CO})_3^+-3\text{-OH-flavone}]^0$ showed almost the same to that of $\text{Re}(\text{CO})_3^+-3\text{-OH-flavone}$, and these results

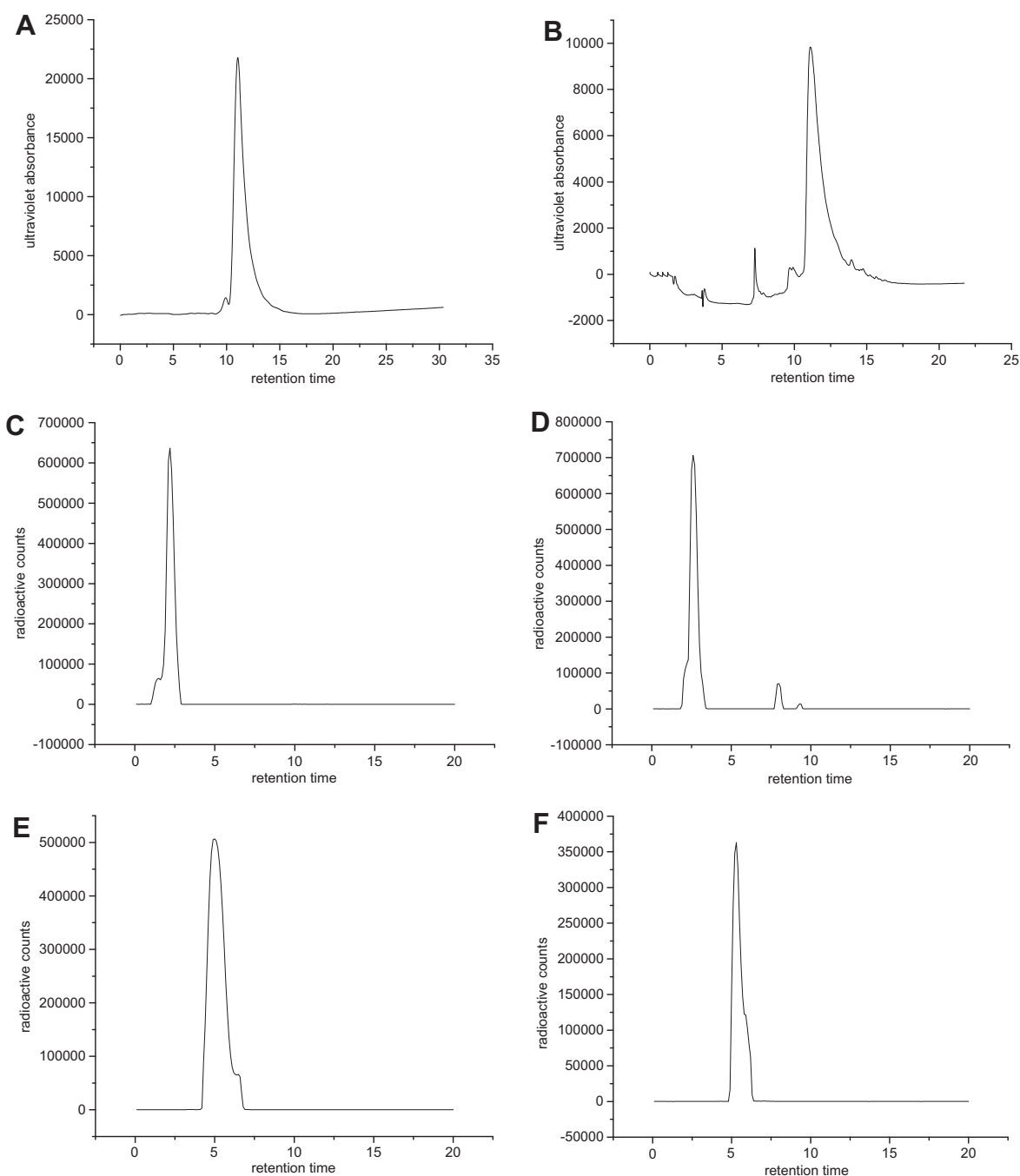


Figure 3. The HPLC chromatograms of compound **C** (A), compound **D** (B), $[^{99m}\text{Tc}(\text{CO})_3^+-6\text{-OH-flavone}]^-$ (C), $[^{99m}\text{Tc}(\text{CO})_3^+-7\text{-OH-flavone}]^-$ (D), $[^{99m}\text{Tc}(\text{CO})_2(\text{NO})^{2+}-6\text{-OH-flavone}]^0$ (E) and $[^{99m}\text{Tc}(\text{CO})_2(\text{NO})^{2+}-7\text{-OH-flavone}]^0$ (F).

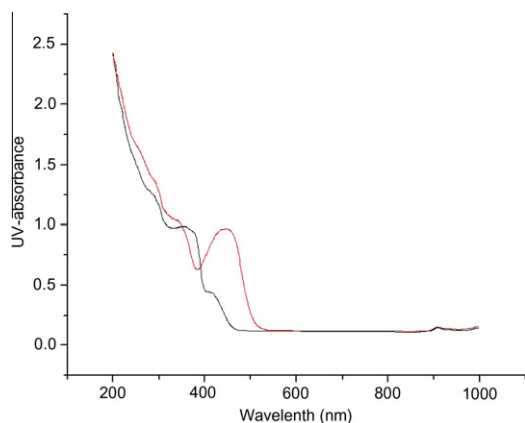


Figure 4. UV-vis absorption spectra (in ethanol solutions) of the ligand (black line) and $\text{Re}(\text{CO})_3^+-3\text{-OH-flavone}$ (red line).

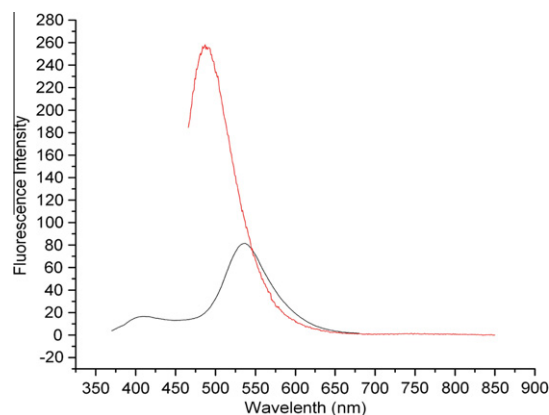


Figure 5. Room temperature fluorescence spectra (in ethanol solutions) of $\text{Re}(\text{CO})_3^+-3\text{-OH-flavone}$ (red line) and 3-OH-flavone (black line).

demonstrated the same structure of $\text{Re}(\text{CO})_3^+-3\text{-OH-flavone}$ and $[\text{}^{99\text{m}}\text{Tc}(\text{CO})_3^+-3\text{-OH-flavone}]^0$.

The preparation of compound **A** was according to²³ and compound **B** was prepared according to Ref. 24. Compound **C** and **D** were synthesized successfully according to^{25b} and the chemical identities of **C** and **D** were confirmed by NMR,²⁶ MS-ESI²⁷ and Infrared Spectrum.²⁸ The labeling yield of $[\text{}^{99\text{m}}\text{Tc}(\text{CO})_3^+-6\text{-OH-flavone}]^-$, $[\text{}^{99\text{m}}\text{Tc}(\text{CO})_3^+-7\text{-OH-flavone}]^-$, $[\text{}^{99\text{m}}\text{Tc}(\text{CO})_2(\text{NO})^{2+}-6\text{-OH-flavone}]^0$ and $[\text{}^{99\text{m}}\text{Tc}(\text{CO})_2(\text{NO})^{2+}-7\text{-OH-flavone}]^0$ detected by TLC²⁹

were higher than 92% according to the labeling methods in,^{25d} and the R_f s of $[\text{}^{99\text{m}}\text{Tc}(\text{CO})_3^+-6\text{-OH-flavone}]^-$, $[\text{}^{99\text{m}}\text{Tc}(\text{CO})_3^+-7\text{-OH-flavone}]^-$, $[\text{}^{99\text{m}}\text{Tc}(\text{CO})_2(\text{NO})^{2+}-6\text{-OH-flavone}]^0$ and $[\text{}^{99\text{m}}\text{Tc}(\text{CO})_2(\text{NO})^{2+}-7\text{-OH-flavone}]^0$ were 0.5–0.6, 0.5–0.6, 0.1 and 0.1, respectively (Table 2). The radio-chemical purities of the Tc complexes were all higher than 95% by reversed phase HPLC.^{30b} Moreover, $[\text{}^{99\text{m}}\text{Tc}(\text{CO})_2(\text{NO})^{2+}-6\text{-OH-flavone}]^0$ and $[\text{}^{99\text{m}}\text{Tc}(\text{CO})_2(\text{NO})^{2+}-7\text{-OH-flavone}]^0$ were proved to be neutral by paper electrophoresis³¹ (Table 3). The retention times for compound C, compound D,

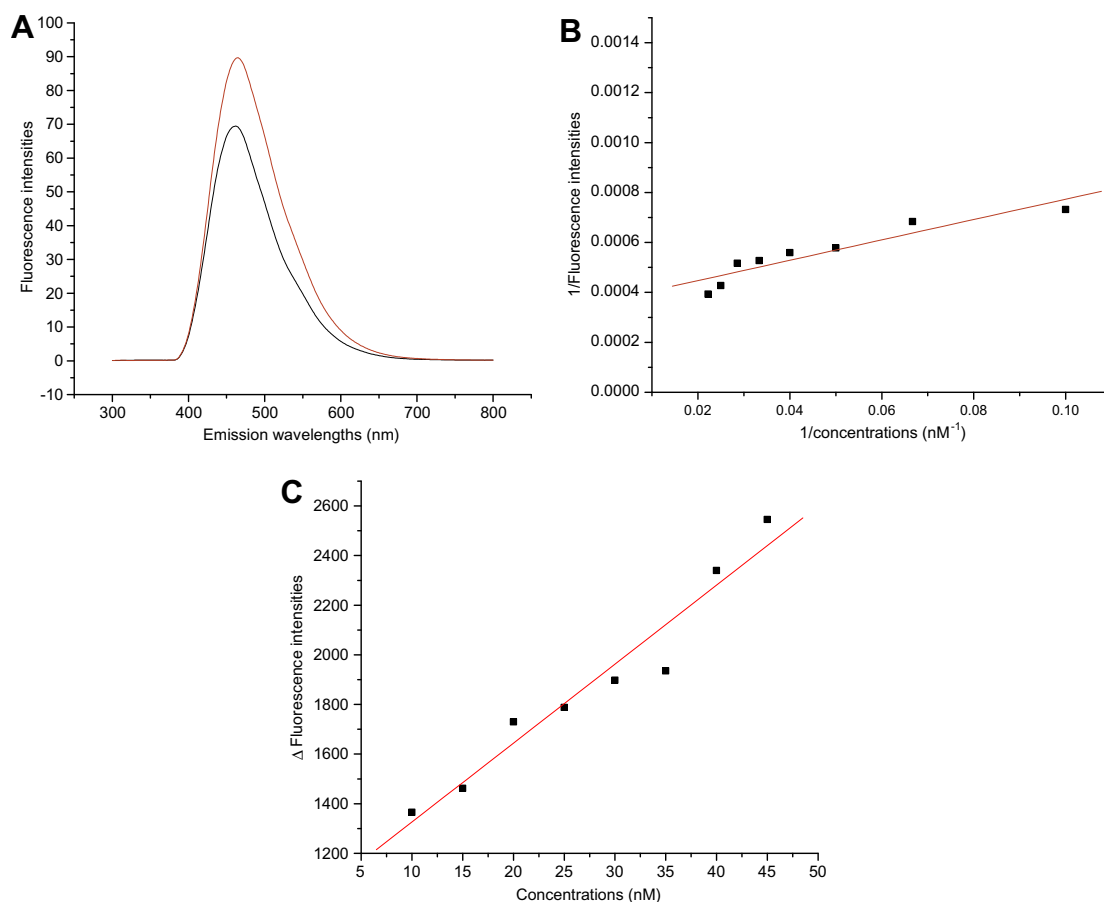


Figure 6. A represents the fluorescence intensities of 45 nM $\text{Re}(\text{CO})_3^+-3\text{-OH-flavone}$ (black line) and the complex incubated with $\text{A}\beta_{(1-40)}$ aggregates (red line); B represents the relationship of the increase of fluorescence intensities and concentrations of $\text{Re}(\text{CO})_3^+-3\text{-OH-flavone}$ incubated with $\text{A}\beta_{(1-40)}$ aggregates; C represents 'Lineweaver-Burk plot'.

Table 4Inhibition and Dissociation constants of compounds binding to aggregates of A β (1–40)

Compounds	Binding affinities		References
	K_d (nM)	K_i (nM)	
Re(CO) $_3^+$ -3-OH-flavone	11.16	—	—
10		22.6	9
11		13.2	9
19		29.0	9
20		72.5	9
6	32.0		10
9	17.5		10
12	8.7		10

[$^{99m}\text{Tc}(\text{CO})_3^+$ -6-OH-flavone] $^-$, [$^{99m}\text{Tc}(\text{CO})_3^+$ -7-OH-flavone] $^-$, [$^{99m}\text{Tc}(\text{CO})_2(\text{NO})^{2+}$ -6-OH-flavone] 0 and [$^{99m}\text{Tc}(\text{CO})_2(\text{NO})^{2+}$ -7-OH-flavone] 0 on UV(radio)-HPLC^{30b} were 11.0, 11.1, 2.2, 2.6, 5.0 and 5.3 min (Fig. 3), respectively.

The spectroscopic properties of the Re(CO) $_3^+$ -3-OH-flavone have been investigated by UV–vis absorption and fluorescence emission properties.³² UV–vis absorption and fluorescence properties were studied on 3-OH-flavone and Re(CO) $_3^+$ -3-OH-flavone. The nature of the auxiliary ligands (i.e., the water, three carbonyl groups and the 3-OH-flavone molecule) were shown to profoundly influence the photophysical behavior of the studied Re(CO) $_3^+$ -3-OH-flavone. Figure 4 shows UV–vis absorption spectra of the investigated species measured in ethanol solution. The spectra of Re(CO) $_3^+$ -3-OH-flavone was characterized by strong absorption centred at

450 nm, different from that of the ligand 3-OH-flavone characterized by high-energy absorption bands at 270–420 nm. It can be assigned as the $\pi \rightarrow \pi^*$ absorption centred mostly in the ligand 3-OH-flavone (spin allowed $S_0 \rightarrow {}^1\text{IL}$ transition) relative to the higher energy bands at 270–420 nm of the UV-absorbance, and the spectral position of the ${}^1\text{IL}$ bands were significantly red-shifted in comparison to the free ligand 3-OH-flavone due to the coordination of the heavy metal Re(I) (tricarbonyl) $^+$ core. The donating character of the Re(CO) $_3^+$ -3-OH-flavone lead to longer wavelengths in comparison to the ligand and demonstrated MLCT absorption band. In fact, the $S_0 \rightarrow {}^1\text{MLCT}$ bands in the UV–vis spectra of the investigated neutral complexes can be seen only as long wavelength tails of the $S_0 \rightarrow {}^1\text{IL}$ transitions. The Re(I) (tricarbonyl) $^+$ complexed with 3-OH-flavone and the ligand under study were fluorescent at room temperature. The fluorescence spectra recorded in ethanol at room temperature were shown in Figure 5. The emission of Re(CO) $_3^+$ -3-OH-flavone was blue-shifted in respect to fluorescence of the corresponding 3-OH-flavone by about 60 nm (from 540 to 480 nm). Moreover, 3-OH-flavone was characterized by strong and weak fluorescence intensity at emission wavelength of 410 and 540 nm, respectively. All the above mentioned findings point to the MLCT character of the room temperature fluorescence (i.e., spin-forbidden $S_0 \leftarrow {}^3\text{MLCT}$ transition), supported also by the big ‘Stokes shifts’ (several thousand cm^{-1}) between emission and absorption maxima (Figs. 4 and 5).

We used the similar method to that of the article published^{19,21} to carry on the binding assays between Re(CO) $_3^+$ -3-OH-flavone and A β aggregates.³³ When A β aggregates was add to the solution of Re

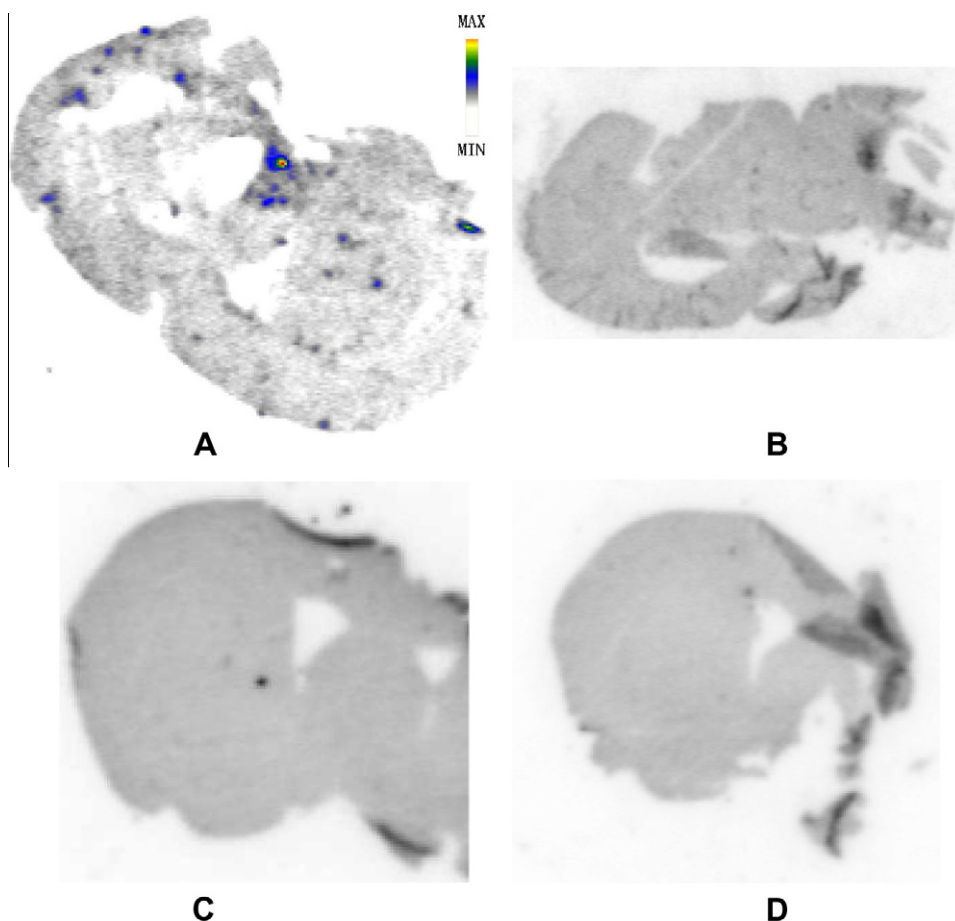


Figure 7. Autoradiography of brain sections from AD mice (Tg C57, APP, PS1 12-month-old) (A) and normal mice (B) labeled with [$^{99m}\text{Tc}(\text{CO})_3^+$ -3-OH-flavone] 0 . A showed that the A β plaques were clearly labeled with the ^{99m}Tc tracer with low background labeling. [$^{99m}\text{Tc}(\text{CO})_2(\text{NO})^{2+}$ -6-OH-flavone] 0 (C) and [$^{99m}\text{Tc}(\text{CO})_2(\text{NO})^{2+}$ -7-OH-flavone] 0 (D) showed the no binding sites in AD mice brain sections.

Table 5Biodistribution of [$^{99m}\text{Tc}(\text{CO})_3^+-3\text{-OH-flavone}$] 0 in normal mice^a

Tissues	5 min	15 min	30 min	60 min	120 min
Brain	0.48 ± 0.05	0.43 ± 0.05	0.49 ± 0.22	0.44 ± 0.08	0.39 ± 0.08
Blood	18.90 ± 3.44	11.09 ± 1.23	11.50 ± 2.89	8.25 ± 1.23	7.51 ± 0.18
Bone	5.54 ± 2.59	4.89 ± 0.68	5.76 ± 1.82	3.92 ± 0.11	3.73 ± 0.38
Muscle	3.38 ± 0.29	2.38 ± 0.35	2.66 ± 0.13	1.88 ± 0.49	1.66 ± 0.48
Kidneys	17.46 ± 0.13	12.95 ± 1.82	13.76 ± 1.07	12.11 ± 1.89	11.20 ± 1.77
Heart	8.53 ± 2.05	5.40 ± 0.12	5.27 ± 0.77	3.43 ± 0.23	3.16 ± 0.40
Spleen	6.65 ± 0.77	4.99 ± 0.66	4.97 ± 0.86	4.40 ± 1.00	4.37 ± 1.17
Lung	16.95 ± 1.45	11.06 ± 3.19	11.37 ± 1.67	9.97 ± 1.34	8.90 ± 0.60
Liver	9.38 ± 0.87	6.32 ± 0.58	8.65 ± 0.91	7.67 ± 0.97	7.25 ± 0.28

^a Expressed as % of injected dose per gram. Each value represents the mean ± SD for 3–4 mice at each interval.

tracer, the fluorescence intensities were increased immediately at the same emission wavelength (Fig. 6A). There was a rather good linear relationship (Eq. 1) between the concentrations of $\text{Re}(\text{CO})_3^+-3\text{-OH-flavone}$ (X) and the increase of fluorescence intensities (Δ fluorescence intensities, Y) when $\text{Re}(\text{CO})_3^+-3\text{-OH-flavone}$ of different concentrations were incubated with $\text{A}\beta_{(1-40)}$ aggregates, respectively (Fig. 6B).

$$Y = 1007.6429 + 31.83029 \times X \quad (1)$$

R: 0.97167, SD: 102.42378, $P < 0.0001$, t -Value: 10.07012, F-Value: 101.40722.

Where Y is fluorescence intensities, X is concentrations, R is linear correlation coefficient, SD is standard deviation.

The linear relationship between the concentrations of $\text{Re}(\text{CO})_3^+-3\text{-OH-flavone}$ (incubated with $\text{A}\beta_{(1-40)}$ aggregates) and fluorescence intensity was analysed using Lineweaver-Burk plot by Microcal Origin 6.0 (Fig. 6C), obtaining (Eq. 2) as below:

$$Y = 3.65643E - 4 + 0.00408 \times X \quad (2)$$

R: 0.93133, SD: 4.54129E-5, P : 7.6833E-4, t -Value: 6.26437, F-value: 39.24234.

Where Y is Δ fluorescence intensities $^{-1}$, X is concentrations $^{-1}$, R is linear correlation coefficient, SD is standard deviation.

According to the (Eq. 2), K_d should be the value of $-X^{-1}$ when the value of Y equalled zero. Thus, $K_d = 0.00408 \times (3.65643E-4)^{-1} = 11.16$ nM. The K_d demonstrated that $\text{Re}(\text{CO})_3^+-3\text{-OH-flavone}$ showed good binding affinity for $\text{A}\beta_{(1-40)}$ aggregates, in comparison to radio-iodide labeled flavone derivatives^{9,10} (Table 4). Although there is no clear mechanism to explain the interaction of small molecules and the $\text{A}\beta_{(1-40)}$ aggregates, according to the research published, we speculate that when Re-tracer inserted to the aggregates, the rotation of the benzene ring in the molecule might be inhibited by the rigidity of the microsurrounding of the aggregates, and this inhibition resulted in a high quantum yield of fluorescence, thus, the increase of the fluorescence intensities occurred.

Autoradiography showed that [$^{99m}\text{Tc}(\text{CO})_3^+-3\text{-OH-flavone}$] 0 could label the plaques in the AD mice (Tg C57, APP, PS1 12-month-old) brain section with low background labeling in comparison to that of the normal mice^{34a} (Fig. 7A and B), oppositely, the two neutral $^{99m}\text{Tc}(\text{CO})_2(\text{NO})^{2+}$ -complexes did not label the AD mice brain sections^{34b} (Fig. 7C and D). These results may be explained that the large-volume $^{99m}\text{Tc}(\text{CO})_2(\text{NO})^{2+}$ -complexes could not insert into the $\text{A}\beta_{(1-40)}$ aggregates. Then, [$^{99m}\text{Tc}(\text{CO})_3^+-3\text{-OH-flavone}$] 0 was examined for biodistribution in normal mice³⁵ (Table 5). [$^{99m}\text{Tc}(\text{CO})_3^+-3\text{-OH-flavone}$] 0 displayed moderate uptake ($0.48 \pm 0.05\%$ ID/g) in the brain at 5 min post-injection, and it displayed slow clearance from the normal brain tissues ($0.39 \pm 0.08\%$ ID/g) at 120 min post-injection. We speculate that the retention of radioactivity in the brain from 5 to 120 min was due to the coordinative H_2O molecule substituted by some other group in the brain, and the substitution resulted in a non-neutral

compound which could not pass through the blood–brain barrier uneventfully, so the Tc molecule washed out slowly from the brain.

In conclusion, we successfully designed and prepared the neutral iso-structural $\text{Re}/^{99m}\text{Tc}(\text{CO})_3^+-3\text{-OH-flavone}$ and the novel $^{99m}\text{Tc}(\text{CO})_2(\text{NO})^{2+}$ -complexes. UV–vis absorption and fluorescence properties were studied on the photophysical behaviors of the ligand and $\text{Re}(\text{CO})_3^+-3\text{-OH-flavone}$. In vitro binding affinity of $\text{Re}(\text{CO})_3^+-3\text{-OH-flavone}$ for $\text{A}\beta_{(1-40)}$ aggregates was up to 11.16 nM by fluorescence spectroscopy, superadd the encouraging results of autoradiography, we concluded that [$^{99m}\text{Tc}(\text{CO})_3^+-3\text{-OH-flavone}$] 0 might be a potential Alzheimer's disease single photon emission tomography imaging agent. However, the structural modification of the coordination compound should be carried on to improve the early brain uptake.

Acknowledgments

This work was financially supported by the Natural Science Foundation of China (No. 20671013); National Basic Research Program of China (No. 2006CB500705).

References and notes

- Cras, P. *Acta. Neurol. Belg.* **1998**, *98*, 186.
- Kung, H. F.; Lee, C. W.; Zhuang, Z. P.; Kung, M. P.; Hou, C.; Plossl, K. J. *Am. Chem. Soc.* **2001**, *123*, 12740.
- Verdile, G.; Fuller, S.; Atwood, C. S.; Laws, S. M.; Gandy, S. E.; Martins, R. N. *Pharmacol. Res.* **2004**, *50*, 397.
- Pike, K. E.; Savage, G.; Villemagne, V. L.; Ng, S.; Moss, S. A.; Maruff, P.; Mathis, C. A.; Klunk, W. E.; Masters, C. L.; Rowe, C. C. *Brain* **2007**, *130*, 2837.
- Boss, M. A. *Biochim. Biophys. Acta* **2000**, *1502*, 188.
- Small, G. W.; Kepe, V.; Ercoli, L. M.; Siddarth, P.; Bookheimer, S. Y.; Miller, K. J.; Lavretsky, H.; Burggren, A. C.; Cole, G. M.; Vinters, H. V.; Thompson, P. M.; Huang, S. C.; Satyamurthy, N.; Phelps, M. E.; Barrio, J. R. *N. Eng. J. Med.* **2006**, *355*, 2652.
- Klunk, W. E.; Engler, H.; Nordberg, A.; Wang, Y. M.; Blomqvist, G.; Holt, D. P.; Bergstrom, M.; Savitcheva, I.; Huang, G. F.; Estrada, S.; Ausen, B.; Debnath, M. L.; Barletta, J.; Price, J. C.; Sandell, J.; Lopresti, B. J.; Wall, A.; Koivisto, P.; Antoni, G.; Mathis, C. A.; Langstrom, B. *Ann. Neurol.* **2004**, *55*, 306.
- Ono, M.; Wilson, A.; Nobrega, J.; Westaway, D.; Verhoeff, P.; Zhuang, Z. P.; Kung, M. P.; Kung, H. F. *Nucl. Med. Biol.* **2003**, *30*, 565.
- Ono, M.; Yoshida, N.; Ishibashi, K.; Haratake, M.; Arano, Y.; Mori, H.; Nakayama, M. *J. Med. Chem.* **2005**, *48*, 7253.
- Ono, M.; Yoshifumi, M.; Ishibashi, K.; Haratake, M.; Nakayama, M. *Bioorg. Med. Chem.* **2007**, *15*, 444.
- Jurisson, S. S.; Lydon, J. D. *Chem. Rev.* **1999**, *99*, 2205.
- Dilworth, J.; Parrot, S. *Chem. Soc. Rev.* **1998**, *27*, 43.
- Zhen, W.; Han, H.; Anguiano, M.; Lemere, C. A.; Cho, C. G.; Lansbury, P. T. *J. Med. Chem.* **1999**, *42*, 2805.
- Dezutter, N. A.; De Groot, T. J.; Busson, R. H.; Janssen, G. A.; Verbruggen, A. M. *J. Labelled Compd. Radiopharm.* **1999**, *42*, 309.
- Dezutter, N. A.; De Groot, T. J.; Bormans, G. M.; Verbruggen, A. M.; Dom, R. J. *Eur. J. Nucl. Med. Mol. Imaging* **1999**, *26*, 1392.
- Serdons, K.; Verduyck, T.; Cleynhens, J.; Terwinghe, C.; Mortelmans, L.; Bormans, G.; Verbruggen, A. *Bioorg. Med. Chem. Lett.* **2007**, *17*, 6086.
- Yang, Y.; Zhang, J. X.; Wang, J. J.; Zhu, L. J. *Radioanal. Nucl. Chem.* **2007**, *273*, 31.
- Klunk, W. E.; Jacob, R. F.; Mason, R. P. *Anal. Biochem.* **1999**, *266*, 667.
- LeVine, H., III *Protein Sci.* **1993**, *2*, 404.
- Voropai, E. S.; Samtsov, M. P.; Kaplevskii, K. N.; Maskevich, A. A.; Stepuro, V. I.; Povarova, b. O. I.; Kuznetsova, I. M.; Turoverov, K. K.; Fink, A. L.; Uverskiid, d.; V.N. *J. Appl. Spectrosc.* **2003**, *70*, 868.

21. Yang, Y.; Zhang, J. X.; Zhu, L.; Zhang, H. *Bioinorg. Chem. Appl.* **2009**, 702730.
22. Alberto, R.; Schibli, R.; Egli, A.; Schubiger, A. P. *J. Am. Chem. Soc.* **1998**, 120, 7987.
23. Yang, Y.; Zhu, L.; Zhang, H. *Acta Crystallogr., Sect. E* **2009**, 65, 3167.
24. Williams, M. A.; Rapoport, H. *J. Org. Chem.* **1993**, 58, 1151.
25. (a) To a aqueous solution of the equimolar mixtures of 3-OH-flavone precursor (15 mg, 0.0625 mmol) and KOH (3.8 mg, 0.0678 mmol), $\text{Re}(\text{CO})_3\text{Br}$ (24 mg, 0.0591 mmol) was added. The mixture was stirred for 5 min at rt, and then heated at 100 °C for 22 h. After cooling to rt, the water was removed under reduced pressure, and the crude product was washed by water for three times to remove the reaction materials, and then the title compound $\text{Re}(\text{CO})_3^+-3\text{-OH-flavone}$ was dried under rt and obtained.
 (b) Synthesis of compound **C** (2,2'-(2-(4-oxo-2-phenyl-4H-chromen-6-yloxy)ethylazanediyldiacetic acid): 6-OH-flavone (361 mg, 1.52 mmol), KOH (85 mg, 1.52 mmol) and **B** (530 mg, 1.52 mmol) were mixed in 100 mL ethanol and stirred at room temperature for 24 h. A white solid precipitated, the mixture was filtered and the filtrates was evaporated off under reduced pressure, and Si-60 was used for final purification: (petroleum ether/ethyl acetate 2:1, R_f : 0.6), the product was obtained as a light yellow solid, then this product (300 mg, 0.59 mmol) and CF_3COOH (67 mg, 0.59 mmol) were mixed in 40 mL CH_2Cl_2 and stirred at room temperature for at least 3 days. The mixture was then washed by saturated NaHCO_3 solution, and the organic phase was evaporated off under reduced pressure, the crude product was obtained as a yellow oil, Si-60 was used for final purification: (petroleum ether/ethyl acetate 2:1, R_f : 0). In addition, the synthesis routes of compound **D** (2,2'-(2-(4-oxo-2-phenyl-4H-chromen-7-yloxy)ethylazanediyldiacetic acid) was the same to that of compound **C**, but 7-OH-flavone was used in stead of 6-OH-flavone.
 (c) $[\text{Re}(\text{CO})_3^+-3\text{-OH-flavone}]^0$ was obtained by heating the aqueous solution of 3-OH-flavone (1 mg/mL) and $[\text{Re}(\text{CO})_3(\text{H}_2\text{O})_3]^+$ moiety (10 mCi/mL) at pH 11 and 100 °C for 40 min.
 (d) $[\text{Re}(\text{CO})_3^+-6\text{-OH-flavone}]^-$ ($[\text{Re}(\text{CO})_3^+-7\text{-OH-flavone}]^-$) were obtained by heating the aqueous solution of compound **C**/compound **D** (0.5 mg/mL) and $[\text{Re}(\text{CO})_3(\text{H}_2\text{O})_3]^+$ moiety (12 mCi/mL) at pH 11 and 100 °C for 100 min. Neutral $[\text{Re}(\text{CO})_2(\text{NO})^{2+}-6\text{-OH-flavone}]^0$ ($[\text{Re}(\text{CO})_2(\text{NO})^{2+}-7\text{-OH-flavone}]^0$) were obtained by heating the aqueous solution of $[\text{Re}(\text{CO})_3^+-6\text{-OH-flavone}]^-$ ($[\text{Re}(\text{CO})_3^+-7\text{-OH-flavone}]^-$) (9 mCi/mL) and NOBF_4 (0.2 mg) at pH 1 and 100 °C for 15 min.
26. NMR spectra were recorded using a Bruker-400 NMR spectrometer with TMS as an internal standard. Coupling constants are reported in hertz. Multiplicity is defined by s (singlet), d (doublet), t (triplet), br (broad), and m (multiplet). $\text{Re}(\text{CO})_3^+-3\text{-OH-flavone}$: ^1H NMR (CDCl_3 , 400 MHz): δ : 8.47 (d, J = 6.8 Hz, 1H), 8.28 (m, 2H), 7.78 (d, J = 7.6 Hz, 1H), 7.71 (m, 3H), 7.53 (m, 2H), 3.51 (s, 2H, $\text{H}_2\text{O-Re}$).
 Compound **C**: ^1H NMR (CDCl_3 , 400 MHz): 7.68 (d, J = 8.4 Hz, 1H), 7.67 (d, J = 5.2 Hz, 1H), 7.47 (m, 5H), 7.55 (s, 1H), 6.77 (s, 1H), 4.26 (t, J = 5.6 Hz, 2H), 3.57 (s, 4H), 3.23 (t, J = 5.6 Hz, 2H). ^{13}C NMR (CDCl_3 , 400 MHz): δ 177.96, 170.78, 163.41, 158.02, 132.17, 132.07, 128.60, 128.47, 126.21, 117.89, 114.93, 107.53, 101.08, 81.15, 68.40, 57.17, 52.96.
 Compound **D**: ^1H NMR (CDCl_3 , 400 MHz): 7.90 (d, J = 4.4 Hz, 2H), 7.67 (dd, J = 4.4 Hz and 5.2 Hz, 2H), 7.64 (d, J = 5.6 Hz, 1H), 7.52 (m, 2H), 7.46 (s, 1H), 7.45 (s, 1H), 6.81 (s, 1H), 4.23 (t, J = 5.2 Hz, 2H), 3.59 (s, 4H), 3.23 (t, J = 5.2 Hz, 2H). ^{13}C NMR (CDCl_3 , 400 MHz): δ 178.22, 170.65, 163.16, 156.23, 133.84, 133.64, 132.16, 128.70, 128.51, 128.45, 126.26, 123.88, 106.88, 81.10, 68.20, 56.91, 53.07.
27. Mass spectra were obtained on Waters Micromass Quattro Micro TM tandem quadrupole mass spectrometer (Micromass Manchester, UK) & LCT Premier XE time-of-flight mass spectrometer (Micromass, Manchester, UK). $\text{Re}(\text{CO})_3^+-3\text{-OH-flavone}$: MS-ESI $^+$ ($^{187/185}\text{Re}$): m/z 550.9 [$\text{M}+\text{Na}$, ^{185}Re] $^+$, 552.8 [$\text{M}+\text{Na}$, ^{187}Re] $^+$.
 Compound **C**: m/z 398.1 [$\text{M}+\text{H}$] $^+$.
 Compound **D**: m/z 788.6 [$2\text{M}+\text{H}$] $^+$, 398.0 [$\text{M}+\text{H}$] $^+$.
28. Infrared spectra were measured on a Nicolet 360 Avatar instrument using a potassium bromide (KBr) disk, scanning from 400 to 4000 cm^{-1} . $\text{Re}(\text{CO})_3^+-3\text{-OH-flavone}$: 3448.2; 2014.1; 1884.6; 1845.6; 1593.4; 1538.6; 1492.8; 1421.7; 1206.0; 1158.1; 752.9; 684.6; 663.7 cm^{-1} .
 Compound **C**: 3381.0; 3056.1; 2961.8; 2925.6; 2855.1; 1683.2; 1634.7; 1437.8; 1376.6; 1184.0; 1120.3; 1045.1; 996.9; 879.8; 746.2; 722.6; 696.4 cm^{-1} .
 Compound **D**: 3444.6; 2924.1; 2849.5; 1733.3; 1630.0; 1459.4; 1430.5; 1375.3; 1252.7; 1091.4; 846.6; 776.9; 724.4 cm^{-1} .
29. Thin layer chromatography was used for the qualitative analysis of every technetium complex. Thin layer chromatography experiments were performed on a polyamide paper (10×0.4 cm) using CH_3CN as a developing solvent. The polyamide strips were left to dry, and the distribution of radioactivity on the strip was determined using a 1470 WizardTM Automatic Gamma Counter.
30. Reversed-phase high-pressure liquid chromatography (RP-HPLC) was performed on an Alltech system with Alltech HPLC pump Model 626, LINEAR UVIS-201, and BIOSCAN flow-counter. The analytic C-18 column (4.6×250 mm, 5 mm particle size, Venusil MP-C18, Agela Technologies Inc., USA). The flow rate was 1 mL/min, A: pure water; B: pure acetonitrile.
 (a) The HPLC analysis gradient was: 0.01–10.00 min, 100% A; 10.01–30.00 min, from 50%A to 100% B; 30.00–40.00 min, 100%B.
 (b) The HPLC analysis gradient was: 0.01–10.00 min, from 100%A to 100% B; 10.01–20.00 min, 100%B.
31. Paper electrophoresis experiments were performed on Xinhua 1# filterpapers (13×1 cm) which were pre-treated with phosphate buffer (pH 7.4). The analyses were carried out using phosphate buffer (pH 7.4) at 150 V for 3 h. The developed paper strips were left to dry; and the distribution of radioactivity on the strip was determined using a 1470 WizardTM Automatic Gamma Counter.
32. Emission spectra were obtained on a Varian Cary Eclipse fluorescence spectrometer.
33. $\text{A}\beta_{(1-40)}$ aggregates were prepared according to the method published previously¹⁸ and used immediately after preparation. Fresh solution (1 μM , 0.5% DMSO/ H_2O) of $\text{Re}(\text{CO})_3^+-3\text{-OH-flavone}$ was diluted to obtain a final concentration range of 15–40 nM in 500 μL PBS (pH 7.4), respectively. Five micro litre solution of $\text{A}\beta_{(1-40)}$ aggregates was added to every 500 μL solution of $\text{Re}(\text{CO})_3^+-3\text{-OH-flavone}$, and incubated for at least 1 min at room temperature before measuring the fluorescence intensity (slit-width: 5 nm; Excitation wavelength was 450 nm, while emission wavelength was 487 nm and a 455–850 nm scan range was performed). All the data were measured and recorded for three times.
34. Film autoradiography: Brain sections from AD mice (Tg C57, APP, PS1 12-month-old) and normal mice were obtained by freezing the brain in powdered dry ice and cut into 20- μm thick sections.
 (a) The AD mice brain section and normal mice brain section were incubated with $[\text{Re}(\text{CO})_3^+-3\text{-OH-flavone}]^0$ (7 $\mu\text{Ci}/1$ mL) for 1.5 h at room temperature, respectively. The sections were then dipped in saturated Li_2CO_3 in 40% EtOH (two 2 min washes) and washed with 40% EtOH (one 2 min wash) followed by rinsing with water for 30 s. After drying, the $^{99\text{m}}\text{Tc}(\text{CO})_3^+$ -labeled sections were exposed to the storage phosphor screen overnight.
 (b) Two different sections from the same AD mice were incubated with $[\text{Re}(\text{CO})_2(\text{NO})^{2+}-6\text{-OH-flavone}]^0$ (8 $\mu\text{Ci}/1$ mL)/ $[\text{Re}(\text{CO})_2(\text{NO})^{2+}-7\text{-OH-flavone}]^0$ (9 $\mu\text{Ci}/1$ mL) for 1 h at room temperature, respectively. The sections were then dipped in saturated Li_2CO_3 in 40% EtOH (two 2 min washes) and washed with 40% EtOH (one 2 min wash) followed by rinsing with water for 30 s. After drying, the two sections were exposed to the storage phosphor screen overnight.
35. Biodistribution in normal mice: All animal biodistribution studies were carried out in compliance with the national laws related to the conduct of animal experimentation with our institutional guidelines and were approved by the Animal Center of Peking University. A saline solution (100 μL) containing radiolabeled agents (20 μCi) was injected directly into the tail vein of normal Kunming mice (18–20 g, 3–4 animals per group). The mice were sacrificed at 5, 15, 30, 60 and 120 min post-injection and the tissues and organs of interest (blood, heart, liver, spleen, lung, kidney, muscle, bone, brain) were collected, wet weighed and counted in a 1470 WizardTM Automatic Gamma Counter. The percentage of injected dose per gram (%ID/g) for each sample was calculated by comparing its activity with that of an appropriate aliquot of the injection solution, the values are expressed as mean \pm 1 standard deviation (SD).